Influence of El Niño on Midtropospheric CO_2 from Atmospheric Infrared Sounder and Model

XUN JIANG AND JINGQIAN WANG

Department of Earth and Atmospheric Sciences, University of Houston, Houston, Texas

EDWARD T. OLSEN

Science Division, Jet Propulsion Laboratory, California Institute of Technology, Pasadena, California

MAOCHANG LIANG

Research Center for Environmental Changes, Academia Sinica, Taipei, and Graduate Institute of Astronomy, National Central University, Jhongli, Taiwan

THOMAS S. PAGANO, LUKE L. CHEN, AND STEPHEN J. LICATA

Science Division, Jet Propulsion Laboratory, California Institute of Technology, Pasadena, California

YUK L. YUNG

Division of Geological and Planetary Sciences, California Institute of Technology, Pasadena, California

(Manuscript received 19 October 2011, in final form 13 January 2012)

ABSTRACT

The authors investigate the influence of El Niño on midtropospheric CO_2 from the Atmospheric Infrared Sounder (AIRS) and the Model for Ozone and Related Chemical Tracers, version 2 (MOZART-2). AIRS midtropospheric CO_2 data are used to study the temporal and spatial variability of CO_2 in response to El Niño. CO_2 differences between the central and western Pacific Ocean correlate well with the Southern Oscillation index. To reveal the temporal and spatial variability of the El Niño signal in the AIRS midtropospheric CO_2, a multiple regression method is applied to the CO_2 data from September 2002 to February 2011. There is more (less) midtropospheric CO_2 in the central Pacific and less (more) midtropospheric CO_2 in the western Pacific during El Niño (La Niña) events. Similar results are seen in the MOZART-2 convolved midtropospheric CO_2, although the El Niño signal in the MOZART-2 is weaker than that in the AIRS data.

1. Introduction

Atmospheric CO_2, an important greenhouse gas in the atmosphere, is increasing globally at a rate of approximately 2 ppm yr^{-1} mainly as a consequence of fossil fuel combustion (Keeling et al. 1995). In addition to the CO_2 trend, atmospheric CO_2 also exhibits strong seasonal cycles. Variations of CO_2 seasonal cycle amplitudes are closely related to carbon exchange with the biosphere (Pearman and Hyson 1980, 1981; Cleveland et al. 1983; Bacastow et al. 1985; Keeling et al. 1996; Buermann et al. 2007). Atmospheric CO_2 also demonstrates intraseasonal and interannual variabilities (Bacastow 1976; Enting 1987; Feely et al. 1987; Keeling and Revelle 1985; Keeling et al. 1995; Dargaville et al. 2000; Dettinger and Ghil 1998; Jiang et al. 2010). Combining satellite/in situ observations and model simulations, we found that there are Madden–Julian oscillation (MJO), semiannual oscillation (SAO), and tropospheric biennial oscillation (TBO) signals in midtropospheric CO_2 (Li et al. 2010; Jiang et al. 2012; Wang et al. 2011). Using midtropospheric CO_2 data from the Atmospheric Infrared Sounder (AIRS), Jiang et al. (2010) found that El Niño–Southern Oscillation (ENSO) can influence midtropospheric CO_2 concentration as the result of a change in the Walker circulation

Corresponding author address: Xun Jiang, Department of Earth and Atmospheric Sciences, University of Houston, 4800 Calhoun Rd., Houston, TX 77004.
E-mail: xjiang7@uh.edu

DOI: 10.1175/JAS-D-11-0282.1

(Julian and Chervin 1978). Midtropospheric CO_2 is enhanced in the central Pacific Ocean and diminished in the western Pacific Ocean during El Niño (Jiang et al. 2010). In the high latitudes, midtropospheric CO_2 concentration can be influenced by the strength of the polar vortex. In this paper, we investigate the temporal variability of midtropospheric CO_2 from AIRS using a multiple regression method, and we compare the results with those from a chemistry-transport model.

2. Data and model

Mixing ratios of midtropospheric AIRS CO_2 are retrieved using the vanishing partial derivative (VPD) method (Chahine et al. 2005, 2008). The maximum sensitivity of AIRS midtropospheric CO_2 is between 500 and 300 hPa. AIRS midtropospheric CO_2 is retrieved globally in the midtroposphere during day and night. AIRS, version 5, CO_2 retrieval products are available at $2° \times 2.5°$ (latitude by longitude) resolution from September 2002 to February 2011. Validation, by comparison to in situ aircraft measurements and retrievals from land-based upward-looking Fourier transform interferometers, demonstrated that AIRS CO_2 is accurate to 1–2 ppm between latitudes 30°S and 80°N (Chahine et al. 2005, 2008). Midtropospheric CO_2 retrieved via the VPD method captures the correct seasonal cycle and trend compared with those from the Comprehensive Observation Network for Trace Gases by Airliner (CONTRAIL) (Chahine et al. 2005).

A three-dimensional (3D) chemistry and transport model, the Model for Ozone and Related Chemical Tracers, version 2 (MOZART-2), was used in this paper to simulate the El Niño signal in midtropospheric CO_2. MOZART-2 is driven by the European Centre for Medium-Range Weather Forecasts Interim (ECMWF-Interim) meteorological data. The horizontal resolution of MOZART-2 is $2.8° \times 2.8°$ (latitude by longitude). There are 45 vertical levels extending up to approximately 50-km altitude (Horowitz et al. 2003). MOZART-2 is built on the framework of the Model of Atmospheric Transport and Chemistry (MATCH). MATCH includes representations of advection, convective transport, boundary layer mixing, and wet and dry deposition. The surface boundary condition for MOZART-2 is the climatological CO_2 surface fluxes from biomass burning, fossil fuel emission, ocean, and biosphere used in Jiang et al. (2008). MOZART-2, driven by the ECMWF-Interim meteorological data and climatological CO_2 surface fluxes, is used to investigate the influence of El Niño on midtropospheric CO_2. To reveal if ECMWF-Interim simulates the ENSO signal well, we have calculated the Southern Oscillation index (SOI) from ECMWF-Interim Re-Analysis datasets by analyzing the standardized mean sea surface pressure differences between Darwin and Tahiti. The SOI derived from ECMWF-Interim correlates well with the standard SOI, which is defined by the sea surface pressure difference between Tahiti and Darwin. The correlation coefficient between two time series is 0.81. The corresponding significance level is 1%. The significance statistics for the correlation are generated by a Monte Carlo method (Press et al. 1992; Jiang et al. 2004). The ECMWF-Interim Re-Analysis captures the ENSO signal well at the surface.

3. Results and discussion

Before exploring the influence of El Niño on midtropospheric CO_2, we first calculated the mean AIRS midtropospheric CO_2 abundance from September 2002 to February 2011. Results for the mean AIRS midtropospheric CO_2 are shown in Fig. 1. There is more midtropospheric CO_2 over the western Pacific and less over the eastern Pacific. This is related to the redistribution of CO_2 as a result of the Walker circulation. There is upwelling air over the western Pacific Ocean, which can bring high values of CO_2 from the surface to the midtroposphere. Air is sinking over the eastern Pacific Ocean, which can bring low concentrations of CO_2 from the high altitude to the midtroposphere.

Next, we investigated the temporal variations of the ENSO signal in midtropospheric CO_2. We calculated the difference of CO_2 between the central Pacific (18°S–18°N, 190°–240°E) and the western Pacific (18°S–18°N, 110°–160°E) areas. A linear trend was removed from the AIRS midtropospheric CO_2 difference. The detrended AIRS midtropospheric CO_2 difference between the central Pacific and the western Pacific is shown by the solid line in Fig. 2a. A linear trend was removed from the standard SOI. The detrended and inverted SOI is shown in Fig. 2a by the dashed line. When there is an El Niño (La Niña) event, the SOI is negative (positive). The CO_2 difference (central Pacific − western Pacific) is positive (negative) for El Niño (La Niña) episodes. It suggests that there is more (less) midtropospheric CO_2 over the central Pacific than over the western Pacific during El Niño (La Niña) episodes. As shown in Fig. 2a, the detrended AIRS CO_2 difference correlates well with the inverted and detrended SOI. The correlation coefficient between the detrended AIRS CO_2 difference and the inverted and detrended SOI is 0.61. The corresponding significance level is 1%. To investigate the interannual variability between the two time series, we applied a low-pass filter to the two time series. The low-pass filter is constructed to keep only signals with periods longer than 15 months. The low-pass filtered CO_2 difference and low-pass filtered and inverted

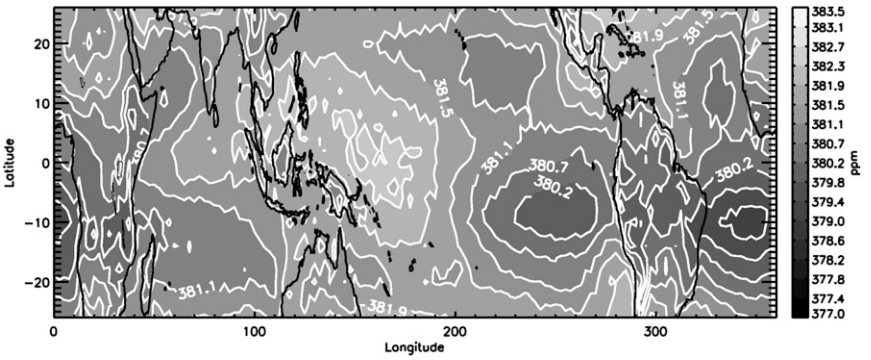

FIG. 1. Mean AIRS midtropospheric CO_2 averaged from September 2002 to February 2011.

SOI are shown in Fig. 2b. The correlation coefficient between the two low-pass-filtered time series is 0.94 (1%).

To better investigate the temporal and spatial variability of the AIRS midtropospheric CO_2 in the tropical region, we applied the multiple regression method to the AIRS midtropospheric CO_2 data. We decomposed AIRS midtropospheric CO_2 concentrations X at each location using the following empirical model:

$$X(t) = A_0 + A_1 N P_1(t/N - 1) + A_2 N^2 P_2(t/N - 1) + A_3 N^3 P_3(t/N - 1) + C_1 \cos(2\pi t) + S_1 \sin(2\pi t) + C_2 \cos(4\pi t) + S_2 \sin(4\pi t) + B \cdot S(t), \quad (1)$$

where t is time; N is the half length of the time period; and P_1, P_2, and P_3 are the first, second, and third Legendre polynomials. The coefficients A_0, A_1, A_2, and A_3 are the mean value, the trend, the acceleration in the trend, and the coefficient for P_3, respectively. We added the third Legendre function to better fit the datasets.

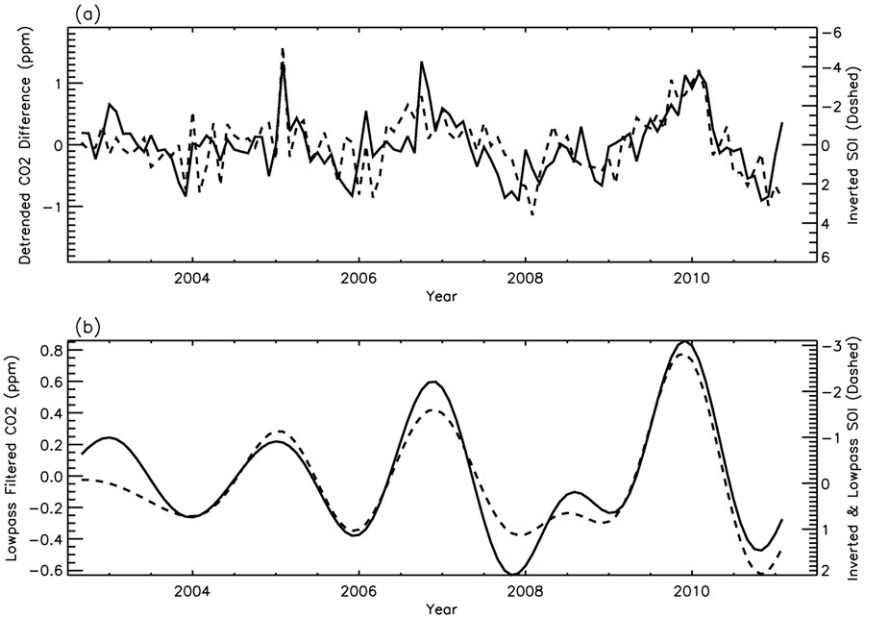

FIG. 2. (a) Differences in the detrended AIRS midtropospheric CO_2 between the central Pacific (18°S–18°N, 190°–240°E) and the western Pacific (18°S–18°N, 110°–160°E) (solid line), and the inverted and detrended SOI (dashed line). Correlation coefficient between the two time series is 0.62 (1% significance level). (b) As in (a), but for low-pass-filtered data. Correlation coefficient between two low-pass-filtered time series is 0.94 (1% significance level).

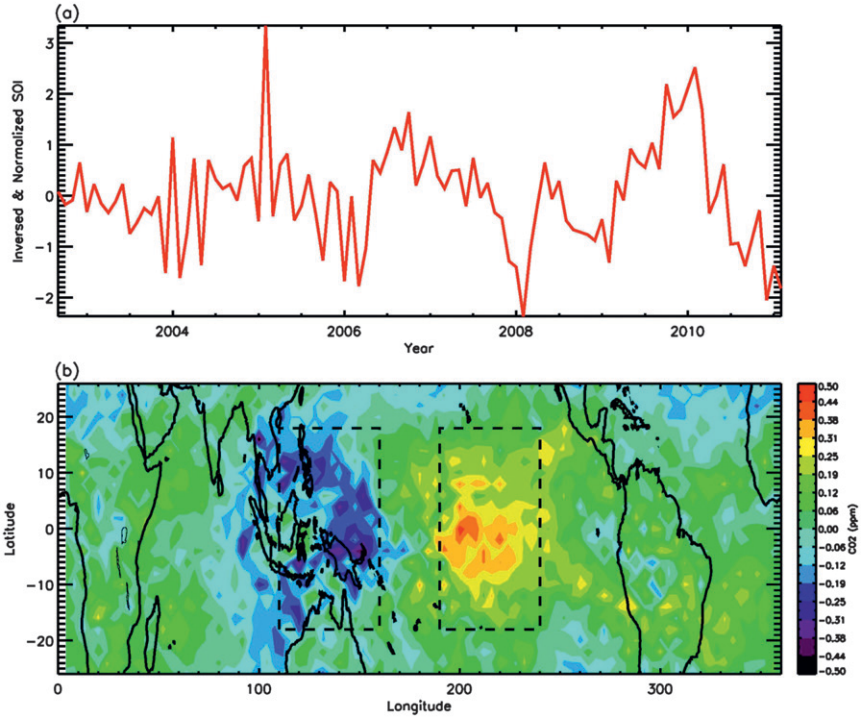

FIG. 3. (a) Inversed, detrended, and normalized SOI. (b) Regression map [coefficient B in Eq. (1)] of the ENSO signal in the AIRS midtropospheric CO_2 in the tropics. Central Pacific (18°S–18°N, 190°–240°E) and western Pacific (18°S–18°N, 110°–160°E) areas used in Fig. 2 are highlighted by dashed boxes in Fig. 3b.

Seasonal and semiannual cycles are represented by the harmonic functions (C_1 and S_1 are the amplitudes of the annual cycle, and C_2 and S_2 are the amplitudes of the semiannual cycle); B is the regression coefficient for the ENSO signal in the midtropospheric CO_2; and $S(t)$ is the inversed, detrended, and normalized SOI index, which is shown in Fig. 3a and was used for regressing the coefficients of ENSO signal in the AIRS midtropospheric CO_2. The standard deviation for the inversed and normalized SOI is 1. Pagano et al. (2011) discussed the midtropospheric CO_2 seasonal cycle from AIRS. We have studied the amplitude and mechanism for the semiannual cycle of the midtropospheric CO_2 in another paper (Jiang et al. 2012). In this paper, we will mainly focus on investigating the influence of ENSO on midtropospheric CO_2.

Regression coefficients for the ENSO signal in the AIRS midtropospheric CO_2 are shown in Fig. 3b. The multiplication of positive (negative) values in Fig. 3a and regression coefficients in Fig. 3b represents the El Niño (La Niño) signal in the AIRS midtropospheric CO_2. There are positive (negative) CO_2 anomalies in the central Pacific and negative (positive) CO_2 anomalies in the equatorial western Pacific during El Niño (La Niña) events. The CO_2 anomaly is about 0.5 ppm in the central Pacific and -0.5 ppm in the western Pacific during El Niño episodes. During strong El Niño cases (e.g., February 2005 and February 2010), the CO_2 amplitude is about 1 to 2 ppm in the central Pacific and -2 to -1 ppm in the western Pacific. During a strong La Niña case (e.g., February 2008), the CO_2 amplitude is about -1 ppm in the central Pacific and 1 ppm in the western Pacific, which is consistent with the results obtained in Jiang et al. (2010).

To investigate how well the model could simulate the ENSO signal in the midtropospheric CO_2, we convolved MOZART-2 CO_2 vertical profiles with the AIRS midtropospheric CO_2 weighting function. MOZART-2 convolved midtropospheric CO_2 differences between the central Pacific and the western Pacific regions were calculated. Detrended MOZART-2 CO_2 differences are shown in Fig. 4a. Detrended model CO_2 differences correlate well with the inverted and detrended SOI index. The correlation coefficient between the two time series is 0.48 (1%). A low-pass filter was applied to the detrended MOZART-2 midtropospheric CO_2 difference and the inverted and detrended SOI (Fig. 4b). The correlation coefficient between two low-pass-filtered time series is 0.65 (1%).

We used the SOI to separate MOZART-2 detrended and deseasonalized CO_2 into two groups. When the SOI

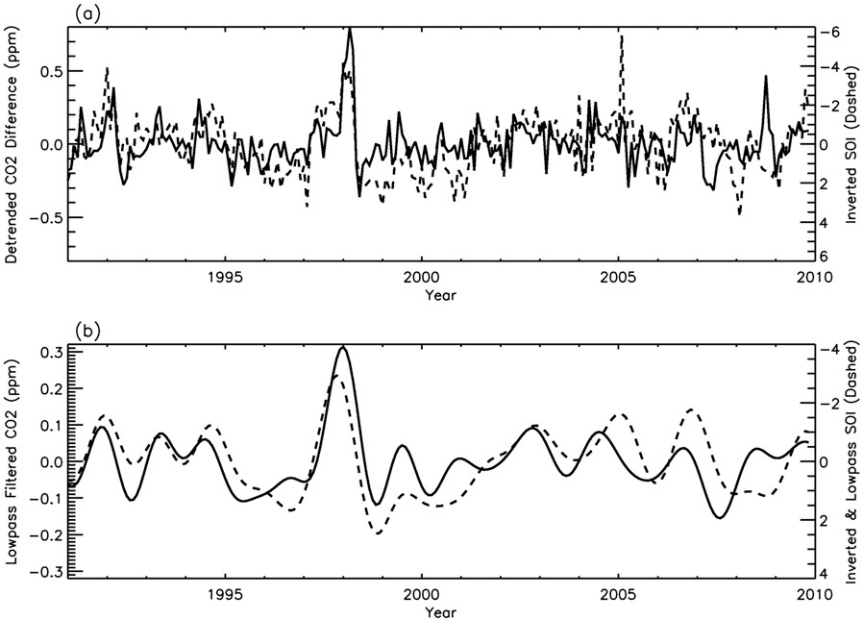

FIG. 4. (a) Differences in the detrended MOZART-2 midtropospheric CO_2 between the central Pacific (18°S–18°N, 190°–240°E) and the western Pacific (18°S–18°N, 110°–160°E) (solid line), and the inverted and detrended SOI (dashed line). Correlation coefficient between the two time series is 0.48 (1% significance level). (b) As in (a), but for low-pass-filtered data. Correlation coefficient between the two low-pass-filtered time series is 0.65 (1% significance level).

was 1.5 standard deviations below (above) the mean value, we considered it to be an El Niño (La Niña) month. MOZART-2 detrended and deseasonalized CO_2 data averaged for 13 El Niño months are shown in Fig. 5a. We also have overlain the vertical velocity in Fig. 5a. During El Niño months, there is rising air over the central Pacific Ocean as shown by the dotted white contours in Fig. 5a. As a result, the surface high CO_2 can be lifted into the midtroposphere over the central Pacific region during El Niño months. A low concentration of midtropospheric CO_2 is seen in the western Pacific Ocean; however, the low CO_2 appears in the subtropical area instead of the tropical area as seen in the AIRS midtropospheric CO_2 (Jiang et al. 2010), which might be related to the relatively weak vertical velocity and relatively strong northward winds over the western Pacific Ocean in the ECMWF-Interim Re-Analysis data. In Fig. 5b, MOZART-2 detrended and deseasonalized CO_2 data for 14 La Niña months suggest that lower CO_2 has been transported from high altitude to the midtroposphere over the central Pacific Ocean. High CO_2 is seen over the western Pacific Ocean; however, the position of the high CO_2 shifts a little bit northward, which might be related to the relatively strong northward winds in the model. Figure 5c presents the MOZART-2 midtropospheric CO_2 differences between the El Niño and La Niña months. The MOZART-2 midtropospheric CO_2 differences (El Niño − La Niña) are about 1 ppm over the central Pacific and −0.7 ppm over the western Pacific. These are consistent with changes in the Walker circulation during El Niño and La Niña months. A Student's t test was used to calculate the statistical significance of the MOZART-2 CO_2 concentration differences during El Niño and La Niña months. The CO_2 differences between El Niño and La Niña months were statistically significant when t was larger than a certain value t_0. CO_2 differences with significance levels less than 5% are highlighted by blue areas in Fig. 5d.

We applied the multiple regression method to the MOZART-2 midtropospheric CO_2. The ENSO component in the MOZART-2 midtropospheric CO_2 is shown in Fig. 6b. There is more (less) midtropospheric CO_2 over the central (western) Pacific Ocean during El Niño months. The amplitude of the ENSO signal in the MOZART-2 midtropospheric CO_2 is about half of the ENSO amplitude in the AIRS midtropospheric CO_2. In addition, the spatial pattern of the ENSO signal in MOZART-2 is different than that from AIRS midtropospheric CO_2 over the western Pacific Ocean. Differences between MOZART-2 and AIRS midtropospheric CO_2 might be related to the climatological surface CO_2 emission and transport used in MOZART-2. In one of our previous studies (Jiang et al. 2008), we found that convection in the 3D models is likely too weak in the

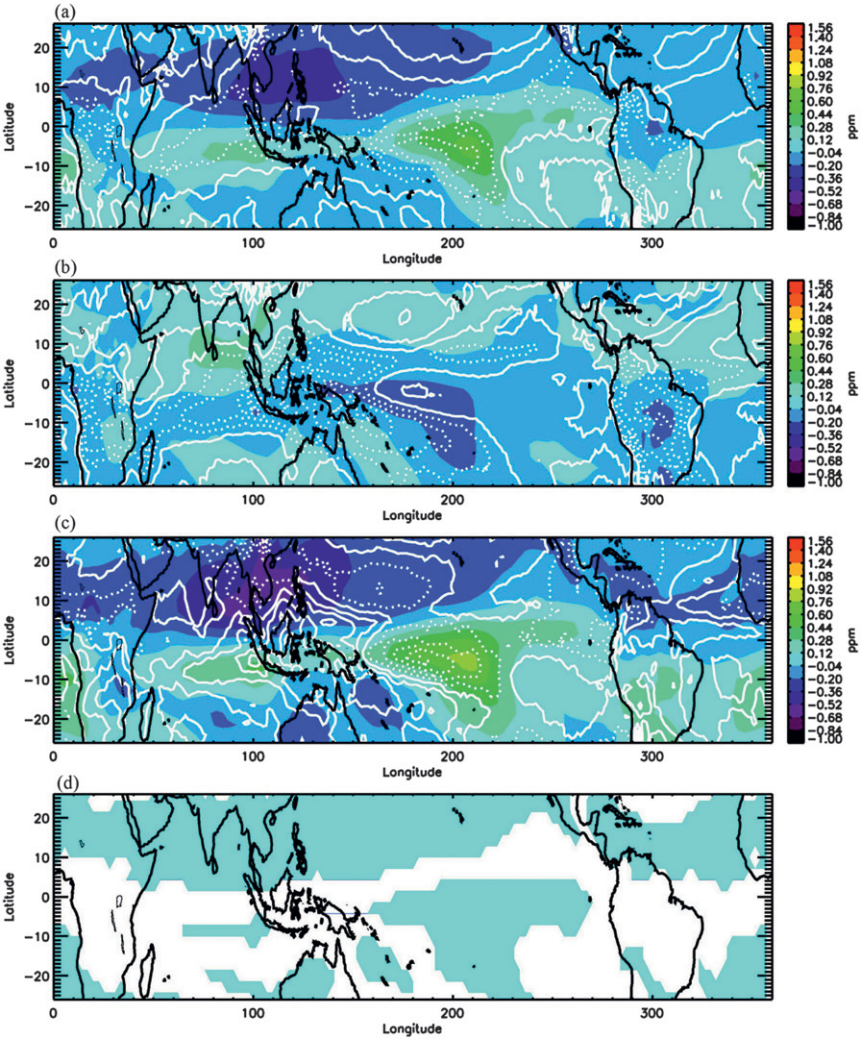

FIG. 5. (a) MOZART-2 detrended and deseasonalized CO_2 (color) and vertical velocities (white contours) averaged for 13 El Niño months. (b) As in (a), but for 14 La Niña months. (c) MOZART-2 CO_2 differences and vertical velocity differences (white contours) between El Niño and La Niña months. (d) MOZART-2 CO_2 differences within a 5% significance level are highlighted in blue. Solid (dotted) white contours refer to sinking (rising) air.

boreal winter and spring. This will lead to underestimation of midtropospheric CO_2 in the models. Similar results were also reported by Yang et al. (2007) when they compared column-averaged dry molar mixing ratios of CO_2 at Park Falls with TransCom simulations. In addition, the strong northward winds in ECMWF-Interim Re-Analysis data might lead to the poor simulation of CO_2 in the western Pacific Ocean. Previous studies suggested that the ocean flux decreases during El Niño events (Feely et al. 1987, 1999). In a sensitivity study, we reduced the CO_2 ocean flux by 20%, and found that the midtropospheric CO_2 decreases by 0.02 ppm. The MOZART-2 CO_2 results might be improved in the future with better surface emission inventories and transport fields.

4. Conclusions

AIRS midtropospheric CO_2 retrievals have been used to investigate the interannual variability of CO_2 in the tropics. Detrended AIRS midtropospheric CO_2 differences between the central and western Pacific correlate well with the inverted and detrended SOI. There is more (less) CO_2 in the central Pacific and less (more) CO_2 in the western Pacific for El Niño (La Niña) events. The multiple regression method was also applied to the AIRS midtropospheric CO_2 in the tropical region. During El Niño episodes, there is more (less) CO_2 in the central (western) Pacific as a result of changes in the Walker circulation. A similar signal was also seen in the MOZART-2

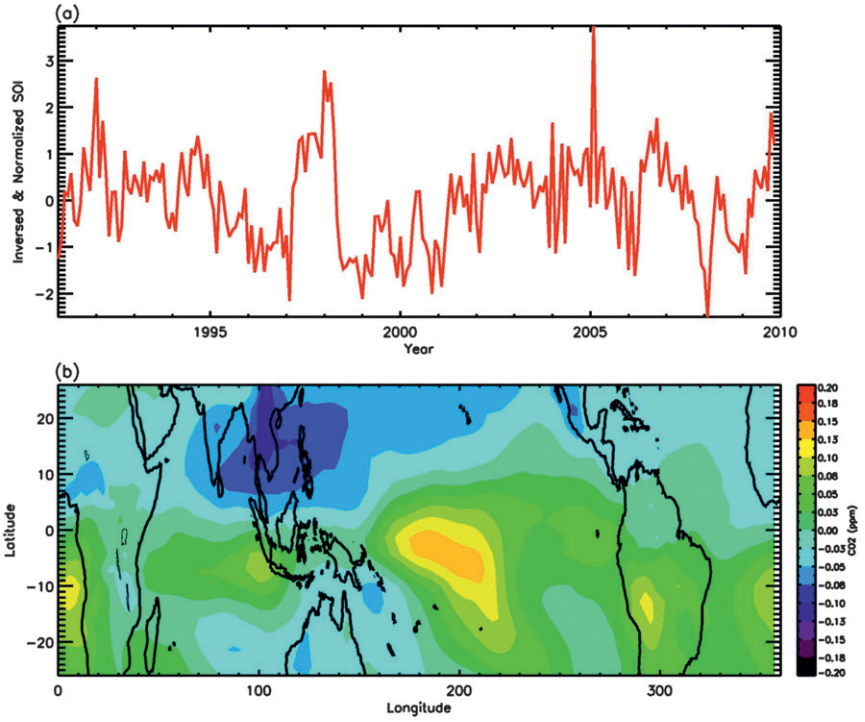

FIG. 6. (a) Inversed, detrended, and normalized SOI. (b) Regression map of the ENSO signal in the MOZART-2 midtropospheric CO_2 in the tropics.

midtropospheric CO_2, although the amplitude and spatial pattern in the model was a little different compared with that in the AIRS midtropospheric CO_2. These results reveal temporal and spatial variability of midtropospheric CO_2 as a response to ENSO. The results may be helpful to modelers who wish to better simulate ENSO signals in the middle troposphere and better constrain vertical transport in the chemistry-transport models. An improved model can be used to better simulate the influence of ENSO on tracers, such as CO_2, CO, O_3, and H_2O.

Acknowledgments. We especially acknowledge Moustafa Chahine, Alexander Ruzmaikin, and Mimi Gerstell, who gave helpful suggestions on this research. XJ was supported by JPL Grant G99694. YLY was supported by the JPL OCO-2 project. Part of this research was carried out at the Jet Propulsion Laboratory, California Institute of Technology, under a contract with the National Aeronautics and Space Administration.

REFERENCES

Bacastow, R. B., 1976: Modulation of atmospheric carbon dioxide by the Southern Oscillation. *Nature,* **261,** 116–118.

——, C. D. Keeling, and T. P. Whorf, 1985: Seasonal amplitude increase in atmospheric CO_2 concentration at Mauna Loa, Hawaii, 1959-1982. *J. Geophys. Res.,* **90,** 10 529–10 540.

Buermann, W., B. Lintner, C. Koven, A. Angert, J. E. Pinzon, C. J. Tucker, and I. Fung, 2007: The changing carbon cycle at the Mauna Loa Observatory. *Proc. Natl. Acad. Sci. USA,* **104,** 4249–4254.

Chahine, M., C. Barnet, E. T. Olsen, L. Chen, and E. Maddy, 2005: On the determination of atmospheric minor gases by the method of vanishing partial derivatives with application to CO_2. *Geophys. Res. Lett.,* **32,** L22803, doi:10.1029/2005GL024165.

——, and Coauthors, 2008: Satellite remote sounding of midtropospheric CO_2. *Geophys. Res. Lett.,* **35,** L17807, doi:10.1029/2008GL035022.

Cleveland, M. S., A. E. Freeny, and T. E. Graedel, 1983: The seasonal component of atmospheric CO_2: Information from new approaches to the decomposition of seasonal time series. *J. Geophys. Res.,* **88** (C15), 10 934–10 946.

Dargaville, R. J., R. M. Law, and F. Pribac, 2000: Implications of interannual variability in atmospheric circulation on modeled CO_2 concentrations and source estimates. *Global Biogeochem. Cycles,* **14,** 931–943.

Dettinger, M. D., and M. Ghil, 1998: Seasonal and interannual variations of atmospheric CO_2 and climate. *Tellus,* **50B,** 1–24.

Enting, I. G., 1987: The interannual variation in the seasonal cycle of carbon dioxide concentration at Mauna Loa. *J. Geophys. Res.,* **92** (D5), 5497–5504.

Feely, R. A., R. H. Gammon, B. A. Taft, P. E. Pullen, L. S. Waterman, T. J. Conway, J. F. Gendron, and D. P. Wisegarver, 1987: Distribution of chemical tracers in the eastern equatorial

Pacific during and after the 1982/1983 ENSO event. *J. Geophys. Res.,* **92** (C6), 6545–6558.

——, R. Wanninkhof, T. Takahashi, and P. Tans, 1999: Influence of El Niño on the equatorial Pacific contribution to atmospheric CO_2 accumulation. *Nature,* **398,** 597–601.

Horowitz, L. W., and Coauthors, 2003: A global simulation of tropospheric ozone and related tracers: Description and evaluation of MOZART, version 2. *J. Geophys. Res.,* **108,** 4784, doi:10.1029/2002JD002853.

Jiang, X., C. D. Camp, R. Shia, D. Noone, C. Walker, and Y. Yung, 2004: Quasi-biennial oscillation and quasi-biennial oscillation-annual beat in the tropical total column ozone: A two-dimensional model simulation. *J. Geophys. Res.,* **109,** D16305, doi:10.1029/2003JD004377.

——, Q. Li, M. Liang, R. L. Shia, M. T. Chahine, E. T. Olsen, L. L. Chen, and Y. L. Yung, 2008: Simulation of upper troposphere CO_2 from chemistry and transport models. *Global Biogeochem. Cycles,* **22,** GB4025, doi:10.1029/2007GB003049.

——, M. T. Chahine, E. T. Olsen, L. Chen, and Y. L. Yung, 2010: Interannual variability of mid-tropospheric CO_2 from Atmospheric Infrared Sounder. *Geophys. Res. Lett.,* **37,** L13801, doi:10.1029/2010GL042823.

——, ——, Q. Li, M. Liang, E. T. Olsen, L. L. Chen, J. Wang, and Y. L. Yung, 2012: CO_2 semiannual oscillation in the middle troposphere and at the surface. *Global Biogeochem. Cycles,* **26,** GB3006, doi:10.1029/2011GB004118.

Julian, P. R., and R. M. Chervin, 1978: A study of the Southern Oscillation and Walker circulation phenomenon. *Mon. Wea. Rev.,* **106,** 1433–1451.

Keeling, C. D., and R. Revelle, 1985: Effects of ENSO on the atmospheric content of CO_2. *Meteoritics,* **20,** 437–450.

——, T. P. Whorf, M. Wahlen, and J. Vanderplicht, 1995: Interannual extremes in the rate of rise of atmospheric carbon dioxide since 1980. *Nature,* **375,** 666–670.

——, J. F. S. Chin, and T. P. Whorf, 1996: Increased activity of northern hemispheric vegetation inferred from atmospheric CO_2 measurements. *Nature,* **382,** 146–149.

Li, K., B. Tian, D. E. Waliser, and Y. L. Yung, 2010: Tropical mid-tropospheric CO_2 variability driven by the Madden–Julian oscillation. *Proc. Natl. Acad. Sci. USA,* **107,** 19 171–19 175, doi:10.1073/pnas.1008222107.

Pagano, T. S., E. T. Olsen, M. T. Chahine, A. Ruzmaikin, H. Nguyen, and X. Jiang, 2011: Monthly representations of mid-tropospheric carbon dioxide from the Atmospheric Infrared Sounder. *Imaging Spectrometry XVI,* S. S. Shen and P. E. Lewis, Eds., International Society for Optical Engineering (SPIE Proceedings, Vol. 8158), doi:10.1117/12.894960.

Pearman, G. I., and P. Hyson, 1980: Activities of the global biosphere as reflected in atmospheric CO_2 records. *J. Geophys. Res.,* **85** (C8), 4468–4474.

——, and ——, 1981: The annual variation of atmospheric CO_2 concentration observed in the northern hemisphere. *J. Geophys. Res.,* **86** (C10), 9839–9843.

Press, W., S. Teukolsky, W. Vetterling, and B. Flannery, 1992: *Numerical Recipes in Fortran 77: The Art of Scientific Computing.* 2nd ed. Cambridge University Press, 933 pp.

Wang, J., and Coauthors, 2011: The influence of tropospheric biennial oscillation on mid-tropospheric CO_2. *Geophys. Res. Lett.,* **38,** L20805, doi:10.1029/2011GL049288.

Yang, Z., R. A. Washenfelder, G. Keppel-Aleks, N. Y. Krakauer, J. T. Randerson, P. P. Tans, C. Sweeney, and P. O. Wennberg, 2007: New constraints on Northern Hemisphere growing season net flux. *Geophys. Res. Lett.,* **34,** L12807, doi:10.1029/2007GL029742.